Theoretical calculations of thermophysical properties of single-wall carbon nanotube bundles*

Miao Ting-Ting(缪婷婷), Song Meng-Xuan(宋梦譞),
Ma Wei-Gang(马维刚), and Zhang Xing(张 兴)†

Key Laboratory for Thermal Science and Power Engineering of Ministry of Education, Department of Engineering Mechanics, Tsinghua University, Beijing 100084, *China*

(Received 20 September 2010; revised manuscript received 28 October 2010)

Carbon nanotube bundles are promising thermal interfacial materials due to their excellent thermal and mechanical characteristics. In this study, the phonon dispersion relations and density of states of the single-wall carbon nanotube bundles are calculated by using the force constant model. The calculation results show that the inter-tube interaction leads to a significant frequency raise of the low frequency modes. To verify the applied calculation method, the specific heat of a single single-wall carbon nanotube is calculated first based on the obtained phonon dispersion relations and the results coincide well with the experimental data. Moreover, the specific heat of the bundles is calculated and exhibits a slight reduction at low temperatures in comparison with that of the single tube. The thermal conductivity of the bundles at low temperatures is calculated by using the ballistic transport model. The calculation results indicate that the inter-tube interaction, i.e. van der Waals interaction, hinders heat transfer and cannot be neglected at extremely low temperatures. For (5, 5) bundles, the relative difference of the thermal conductivity caused by ignoring inter-tube effect reaches the maximum value of 26% around 17 K, which indicates the significant inter-tube interaction effect on the thermal conductivity at low temperatures.

Keywords: single-wall carbon nanotube bundles, van der Waals interaction, specific heat, thermal conductivity

PACS: 65.80.–g, 63.22.Gh, 61.48.De, 34.20.Cf **DOI:** 10.1088/1674-1056/20/5/056501

1. Introduction

Since the discovery of the carbon nanotubes (CNTs) in 1991 by Iijima,[1] the scientific community has displayed a growing interest in this allotropic form of carbon because of their remarkable thermal, electrical and mechanical properties.[2] The properties of single-wall and multi-wall CNTs, which are determined by how many graphene planes are coaxially assembled, have been reported extensively in recent years. Experimentally, Kim *et al.*[3] first carried out a measurement of the thermal conductivity of a multi-wall CNT (MWCNT) by using a microfabricated suspended device and the observed value is more than 3000 $\mathrm{W\cdot m^{-1}\cdot K^{-1}}$. Fujii *et al.*[4] measured the thermal conductivity of a single MWCNT by using a novel sample-attached T-type nanosensor and the maximum value exceeds 2000 $\mathrm{W\cdot m^{-1}\cdot K^{-1}}$. Pop *et al.*[5] extracted the thermal conductivity of a single-wall CNT (SWCNT), more than 3000 $\mathrm{W\cdot m^{-1}\cdot K^{-1}}$, from its high-bias ($I$–$V$) electrical characteristics by the Joule self-heating. Theoretically, Berber *et al.*[6] reported an ultrahigh thermal conductivity, 6600 $\mathrm{W\cdot m^{-1}\cdot K^{-1}}$, of an isolated (10, 10) SWCNT at room temperature, calculated by molecular dynamics simulations. The thermal conductivity of an SWCNT changed with the tube lengths was studied by Maruyama *et al.*[7] Mingo and Broido[8] proposed quantum-mechanical ballistic thermal conductance of SWCNT to answer how high for the ballistic lattice thermal conductance and how long for a sample that remains the ballistic phonon transport. Recently, Lindsay *et al.*[9] studied the phonon thermal transport and intrinsic lattice thermal conductivity in SWCNTs beyond the relaxation approximation and phonon-phonon scattering selection rules. Moreover, CNTs are also a good additive for enhancing the base fluids. Choi *et al.*[10] have found that dispersion of a very small amount of nanotubes into synthetic poly (α-olefin) oil produced a remarkable change in the effective thermal conductivity of the base fluid with the thermal conductivity ratio exceeding 2.5 at 1 vol % nanotubes.

Differing from MWCNTs, SWCNTs usually self-assemble into a two-dimensional hexagonal close-

*Project supported by the National Natural Science Foundation of China (Grant Nos. 50730006 and 50976053).
†Corresponding author. E-mail: x-zhang@tsinghua.edu.cn
© 2011 Chinese Physical Society and IOP Publishing Ltd

packed lattice forming bundles, typical of van der Waals interactions. Based on some researchers' excellent works[11−14] on the synthesis of massive arrays of monodispersed CNTs, the CNT bundles have emerged as a promising next-generation thermal interface solution in a variety of thermal management applications. For example, integrated circuits are subjected to tight thermal budgets to maintain acceptable reliability standards. Several groups have measured the thermal properties of the bundles. Hone *et al.*[15] reported that the thermal conductivity of the SWCNT bundles in the parallel direction exceeds 200 $\mathrm{W}\cdot\mathrm{m}^{-1}\cdot\mathrm{K}^{-1}$. Xu and Fisher[16] have measured the effective thermal conductivity of the CNTs sample by using a 3-omega method and the measured value was 74 to 83 $\mathrm{W}\cdot\mathrm{m}^{-1}\cdot\mathrm{K}^{-1}$, one order higher than that of the best thermal greases or phase change materials. Although the thermal properties are better than those of conventional thermal interfacial material, we can find that the effective thermal conductivity of the bundles greatly decreases in comparison with the corresponding single tube. Hence, it is of special interest to study the underlying mechanisms.

It is well known that graphite represents the reference state of any type of CNT. The graphene planes hold together with a strong C–C bond. Differing from the isolated tube, besides the C–C bond interactions, the bundles are held together with van der Waals force, which is a non-bonded interaction and can be either an attraction or repulsion. In this paper, to study the thermal properties of the SWCNT bundles and the attribution of inter-tube interactions on the heat transport, the van der Waals force is taken into account by using the general Lennard–Jones "6–12" potential. A force constant model is developed to calculate the phonon dispersion relations (PDR) and density of states (DOS) of the SWCNT bundles, which are on the basis of generating an SWCNT bundle. Based on the calculated PDR, the specific heat and the low-temperature thermal conductivity of the SWCNT bundles are calculated. The results show that both the specific heat and thermal conductivity decrease at low temperatures in comparison with those of single tube, which illustrates the effect of the inter-tube van der Waals interaction on the thermal properties of bundles.

2. Phonon dispersion relations and density of states

In this study, the (5, 5) SWCNT bundle is selected as a representation to be studied. As shown in Fig. 1, the core SWCNT has six nearest neighbours,[17,18] with the inter-tube spacing 0.32 nm. The nanotubes of the bundles are remarkably uniform in diameter and tens to hundreds of micrometers in length.[19] The vector (5, 5) denotes the chirality of the bundles, which is determined by the corresponding isolated SWCNTs. From the structural point of view, CNTs can be taken as single sheets of graphite, rolled into a cylindrical shape with axial symmetry. The "rolling up" of the graphene sheet is described by the chiral vector which can be expressed as $\boldsymbol{C}_\mathrm{h} = n\boldsymbol{a}_1 + m\boldsymbol{a}_2 \equiv (n, m)$, where integers n and m represent the chiral indices and $|\boldsymbol{a}_1| = |\boldsymbol{a}_2| = 2.49$ Å is the lattice constant of graphite. Special cases are 'zigzag' (n, 0) and 'armchair' (n, n), i.e., (5, 5) nanotubes.

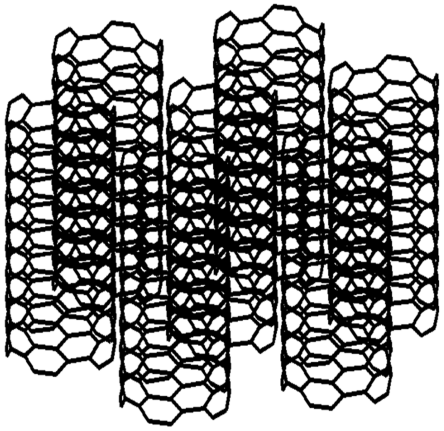


Fig. 1. The calculation generated structure of the (5, 5) SWCNT bundle.

An approach is developed to calculate the phonon dispersion relations with a force constant model,[20] in which the inter-atomic forces are represented by spring constants. Although the model is simple, the experimental results can be reproduced as closely as possible by increasing the number of force constants.

In general, the equation of lattice motion for the displacement of the $\kappa^{\overline{\mathrm{th}}}$ atom in the $i^{\overline{\mathrm{th}}}$ unit cell is given by

$$M_\kappa \frac{\mathrm{d}^2\boldsymbol{u}_{i\kappa}}{\mathrm{d}t^2} = -\sum_{j\nu} \boldsymbol{K}_{i\kappa,j\nu}\boldsymbol{u}_{j\nu}, \tag{1}$$

where $i\kappa$, $j\nu$ denotes the $\kappa^{\overline{\mathrm{th}}}$ atom in the $i^{\overline{\mathrm{th}}}$ unit cell and the $\nu^{\overline{\mathrm{th}}}$ atom in the $j^{\overline{\mathrm{th}}}$ unit cell, respectively and M_κ is the mass of the $\kappa^{\overline{\mathrm{th}}}$ atom. It is supposed that

each atom is displaced from its equilibrium position by an amount $\boldsymbol{u}$. The $\boldsymbol{K}_{i\kappa,j\nu}$ represents the 3×3 force constant tensor between the $\kappa^{\overline{\text{th}}}$ and the $\nu^{\overline{\text{th}}}$ atoms. It is the second-order derivatives of the potential energy, i.e.

$$\boldsymbol{K}_{i\kappa,j\nu} = \frac{\partial^2 E}{\partial \boldsymbol{u}_{i\kappa} \partial \boldsymbol{u}_{j\nu}}. \tag{2}$$

According to periodic solutions of Eq. (1), the set of simultaneous equations is given by

$$\omega^2(\boldsymbol{k}) \cdot \boldsymbol{u}_\kappa(\boldsymbol{k}) = \sum_\nu \boldsymbol{D}_{\kappa\nu}(\boldsymbol{k}) \boldsymbol{u}_\nu(\boldsymbol{k}), \tag{3}$$

where ω is the phonon angular frequency, $\boldsymbol{k}$ is the wave vector of the vibrational wave, $\boldsymbol{D}_{\kappa\nu}(\boldsymbol{k})$ is a $3N\times3N$ dynamical matrix, which denotes the interaction between the κ^{th} and the ν^{th} atoms and N is the number of atoms in an unit cell. The matrix $\boldsymbol{D}_{\kappa\nu}(\boldsymbol{k})$ is

$$\begin{aligned} &\boldsymbol{D}_{\kappa\nu}(\boldsymbol{k}) \\ &= \frac{1}{\sqrt{M_\kappa M_\nu}} \sum_{R_i - R_j} \boldsymbol{K}_{i\kappa,j\nu} \cdot \exp\left[\mathrm{i}\boldsymbol{k}(\boldsymbol{R}_i - \boldsymbol{R}_j)\right]. \end{aligned} \tag{4}$$

The condition for the set of linear homogeneous Eq. (3) to possess a nontrivial solution is

$$\det\left[\omega^2(\boldsymbol{k})\boldsymbol{\delta}_{\kappa\nu} - \boldsymbol{D}_{\kappa\nu}(\boldsymbol{k})\right] = 0. \tag{5}$$

Equation (5) determines the relation of phonon angular frequency and wave vector $\boldsymbol{k}$, which is called the phonon dispersion relation. To solve Eq. (5), the eigenvalues of the dynamical matrix need to be solved. For the SWCNT bundles, the force constant matrix of two atoms is

$$\begin{aligned} \boldsymbol{K}_{i\kappa,j\nu} &= \frac{\partial^2 (E_{\text{in}} + E_{\text{int}})}{\partial \boldsymbol{u}_{i\kappa} \partial \boldsymbol{u}_{j\nu}} \\ &= \frac{\partial^2 E_{\text{in}}}{\partial \boldsymbol{u}_{i\kappa} \partial \boldsymbol{u}_{j\nu}} + \frac{\partial^2 E_{\text{int}}}{\partial \boldsymbol{u}_{i\kappa} \partial \boldsymbol{u}_{j\nu}}, \end{aligned} \tag{6}$$

where E_{in} denotes the potential energy in one tube and E_{int} indicates the inter-tube interaction potential energy. Force constant of the in-tube part $\partial^2 E_{\text{in}}/\partial \boldsymbol{u}_{i\kappa} \partial \boldsymbol{u}_{j\nu}$ corresponds to that of an individual single-walled CNT. It can be obtained by Satio's[21] approach to calculating the SWCNT phonon dispersion relation.

The interaction between tubes is van der Waals force and the potential energy of two atoms, $V(r)$, is the function of interatomic distance r and is usually denoted by the Lennard–Jones (LJ) mode

$$V(r) = 4\varepsilon \left[\left(\frac{\sigma}{r}\right)^{12} - \left(\frac{\sigma}{r}\right)^{6} \right]. \tag{7}$$

The values chosen for van der Waals parameters are $\varepsilon = 0.002964$ eV and $\sigma = 3.407$ Å.[22] According to Eq. (7), the inter-tube potential energy E_{int} can be determined by taking a sum of all atom pairs in the adjacent tubes. Substituting the calculated potential energy into Eq. (6), we can obtain the force constant.

The effect of inter-tube interactions on the phonons of SWCNT was first discussed by Venkateswaran *et al.*[23] Later on, several groups achieved an estimation of the influence of these interactions on the frequencies of the Raman modes.[24] So far, all calculations were performed by assuming that the bundle lattice is composed of identical (same diameter, same orientation) and infinitely long nanotubes. The LJ potential described by Eq. (7) is applied to account for van der Waals inter-tube interactions. The tubes are supposed to keep circular and the effect of inter-tube interactions on the tube shape at equilibrium can be neglected. This assumption has been justified on tubes of diameter smaller than 3 nm.[25,26]

Figure 2 shows the phonon dispersion curves for a (5, 5) bundle. The Γ–X is the k-space direction parallel to the nanotube axis, while the dispersion relations for wave vectors perpendicular to the nanotube axis are shown in the Γ–M portion. It can be seen that the axial vibration mode is close to that of a single SWCNT, while most of the radial phonon dispersion curves are level line, except for a few curves in extremely low frequency region. Comparing the PDR of the isolated (5, 5) tube and that of the corresponding bundles in Fig. 3, we can find very weak changes of the mode frequencies in high frequency range, while significant frequency shifts appear in low frequency range. Therefore, the enlarged comparison of the axial direction phonon dispersion relations near the Brillouin zone centre is also presented in Fig. 3. The selected low-frequency modes, including the four acoustic modes and two lowest optical modes: a longitudinal acoustic mode (LA), doubly degenerated transverse acoustic modes (TA), a twisting mode (TW) and doubly degenerated radial breathing mode (R), display a strong dispersion along the direction normal to the tube axis. A significant effect of the inter-tube interactions is that the $k = 0$ TW (rigid rotation around the tube axis) shifts to non-zero frequency and its frequency increases significantly in comparison with that of single tube. The R modes exhibit a slight change due to their radial character, while the LA and TA modes do not change obviously.

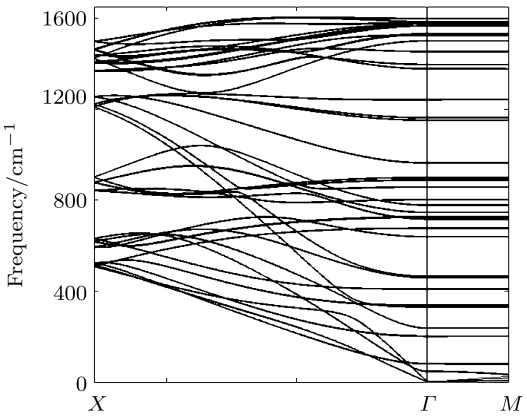


Fig. 2. Phonon dispersion relations curves for (5, 5) SWCNT bundle.

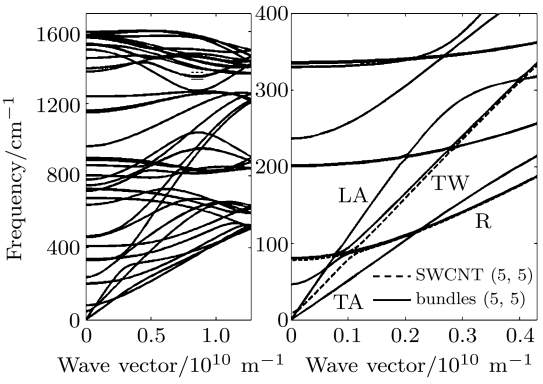


Fig. 3. Comparison of the low-frequency PDR between an isolated tube and bundle.

The phonon DOS for bundles and that of the corresponding isolated tube are compared in Fig. 4. Coinciding well with the previous PDR analysis, the profile of the bundle DOS is close to that of an isolated tube in the high frequency region. In contrast, significant changes are observed at low frequencies, as emphasized on the enlarged graph of Fig. 4. As expected,

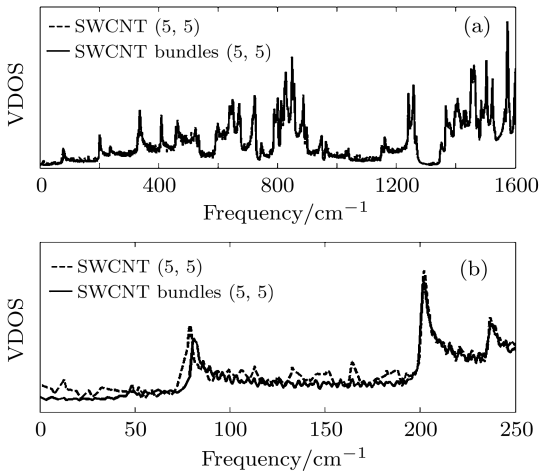


Fig. 4. The comparison of vibrational density of state (VDOS) for isolated tube and bundles. (a) The full frequency band, (b) the low frequency band.

in bundles, the singularity at zero frequency due to the one dimensional (1D) character of isolated tubes disappears when inter-tube interactions are accounted for. On the other hand, the entire phonon spectrum shifts to higher frequency in the low frequency region and consequently leads to decreasing number of low-frequency phonon.

3. Specific heat

The thermal properties of SWCNT bundles, including specific heat and thermal conductivity, strongly depend on the phonon dispersion relations and phonon density of states.

The specific heat, in principle, consists of contributions from both phonons and electrons. However, for 3D crystalline graphite and 2D graphite layers, from which CNTs are derived, the dominant contribution to the specific heat comes from the phonons. Hence, the specific heat of SWCNT bundles is also expected to be dominated by phonons. In general, the phonon contribution to the specific heat can be written as

$$C_V = \frac{1}{M_{\text{tube}}} \sum_{k,p} \frac{k_{\text{B}} x^2 \cdot \exp(x)}{[\exp(x) - 1]^2}, \quad x = \frac{\hbar\omega}{k_{\text{B}} T}, \quad (8)$$

where M_{tube} is the mass of CNT, $\hbar$ is Planck constant, k_{B} is Boltzmann constant, p is vibrational modes and T is temperature.

According to the phonon dispersion relations previously obtained, the specific heat of the SWCNT bundles is calculated from Eq. (8). To verify the applied calculation method, specific heat of an isolated tube is calculated first based on the corresponding PDR, as shown in Fig. 5. The profile shows that the calculated curve agrees well with the experimental data.[27] It can be found that the specific heat increases with the increase of temperature and then tends to a constant. This is due to the fact that more phonon states are occupied at higher temperature. At extremely low temperature, the dominant contribution to the specific heat comes from the four acoustic modes discussed above. When the temperature increases slightly (∼30 K), the linear relationship between specific heat and temperature is no longer maintained since the optical branch begins to contribute to the specific heat. As temperature continues to rise, more and more optical branches contribute to specific heat. The exponent of the power-law dependence of the specific heat and the temperature gradually transits from one to two. Moreover, according to

the Dulong–Petit law, when the temperature increases much greater than the Debye temperature, the phonon heat capacity of solid will tend to a constant and is independent of temperature and material properties. Figure 5 also compared the specific heat of bundles and that of the isolated nanotube. As can be seen, the specific heat of SWCNT bundles exhibit a slight reduction at extremely low temperatures in comparison with that of the single tube. The reason is that the low frequency acoustic phonons make a significant contribution to specific heat at extremely low temperature. As illustrated above, on account of the van der Waals interaction, the entire phonon spectrum of the bundles shifts to a higher frequency and the number of the low frequency phonon decreases, which leads to a slight reduction to the specific heat of bundles. On the other hand, the specific heat of the single tube and the bundles are overlapping approximately above 50 K, which illustrates that the influence of inter-tube interaction on the specific heat of bundles is mainly at very low temperatures. Therefore, the effect of van der Waals interaction on the specific heat of bundles can be neglected except at extremely low temperature. The specific heat of bundles is more reflected by the isolated tube itself.

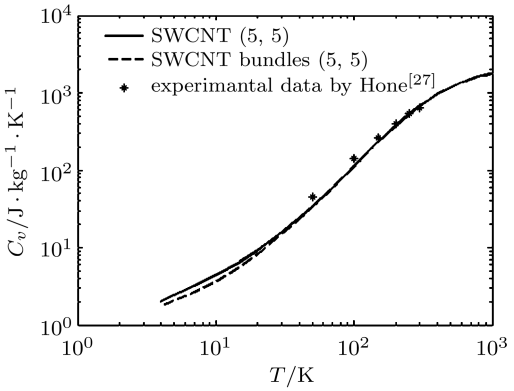


Fig. 5. The calculated specific heat versus temperature curves.

4. Thermal conductivity

The thermal conductivity can be extracted through

$$\lambda = G \cdot L/S, \tag{9}$$

where G is the thermal conductance, L is the length of the tube and S is the cross section. In this paper, we investigate the low-temperature thermal conductance of bundles through a theoretical analysis based on the Landauer theory of heat transport by Takahiro *et al.* The thermal conductance is given as[28]

$$G = \frac{k_{\mathrm{B}}^2 T}{2\pi\hbar} \sum_p \int_{x_p^{\min}}^{x_p^{\max}} x^2 \, \mathrm{e}^x / (\mathrm{e}^x - 1)^2 \eta \, \mathrm{d}x, \tag{10}$$

where $x_p^\gamma = \hbar\omega_p^\gamma / k_{\mathrm{B}}T$, γ denotes 'min' or 'max', $\omega_p^{\min}$ and $\omega_p^{\max}$ are the minimum and maximum angular frequencies of the $p^{\overline{\mathrm{th}}}$ phonon dispersion, respectively and η is the phonon transmissivity, which reflects the effect of phonon scattering on the thermal conductance. The focus of this study is on the thermal conductance of CNT at low temperatures, where the phonon mean free path is sufficiently large in comparison with the dimensions of the CNT. Hence, other scatterings, i.e., lattice defection scattering, can be ignored and heat transfer will be solely in the form of ballistic transport, namely $\eta = 1$. The thermal conductance in CNTs can be determined by substituting $\omega_p^{\min}$ and $\omega_p^{\max}$ for all phonon modes p into Eq. (10). The phonon dispersion relation can be obtained by diagonalizing the dynamical matrix constructed with the scaled force-constant model discussed above. The quantization of thermal conductance originates from low-energy excitations of long-wavelength acoustic phonons and the two lowest optical modes at sufficiently low temperatures. Therefore, taking into account the four acoustic and two lowest optical modes and substituting the values of $\omega_p^{\min}$ for these branches at the Γ point into the formula of Eq. (10), we can give the thermal conductance. For the ballistic transport model, the limitation of the tube length should be less than the phonon mean free path. Single-wall CNTs, which are natural quantum wires of small size and high stiffness, have a large phonon mean free path of the order of 1 μm.[29,30] Therefore, the length of the tube is taken as $L = 1$ μm. The cross section is calculated by $S = \pi d\Delta$, where d is the diameter, and Δ is the thickness of the SWCNT determined from experiment, ∼0.335 nm.

Figure 6 presents the low temperature-dependent thermal conductivity calculated by the ballistic transport model. It can be found that the low-temperature thermal conductivity of CNTs is linearly dependent on temperature, which implies the existence of quantized thermal conductance in CNTs. The quantization of thermal conductance originates from low-energy excitations of long-wavelength acoustic phonons (four branches in Fig. 3) at temperatures sufficiently low such that the two lowest optical modes with an energy

gap are not excited. Moreover, Figure 6 also displays the comparison of isolated single-wall tube and bundles with the same chiral vector (5, 5). The thermal conductivity of the bundles decreases significantly in comparison with that of the single tube. According to Bose–Einstein distribution, at low temperatures, the low-frequency phonon dominates the heat transport process. As illustrated in Fig. 4, the inter-tube interaction in bundles increases the phonon frequency and consequently reduces the low-frequency phonon number, which leads to decreasing thermal conductivity of bundles. To illustrate the effect of inter-tube interaction on the bundles thermal conductivity more clearly, the relative differences of the thermal conductivity with and without inter-tube interaction are shown in Fig. 7. It can be found that the relative difference rises rapidly at extreme low temperatures first and reaches the maximum value 26% around 17 K, and then decreases and tends to 17.5% at higher temperature. Therefore, the effect of van der Waals interaction on the thermal conductivity at low temperature cannot be neglected.

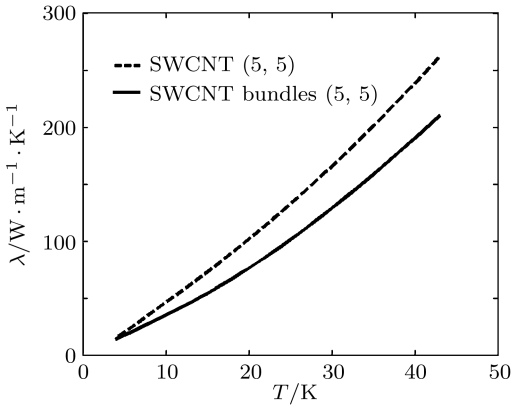


Fig. 6. Low temperature-dependent thermal conductivity of the isolated tube and bundles with the same chiral vector (5, 5).

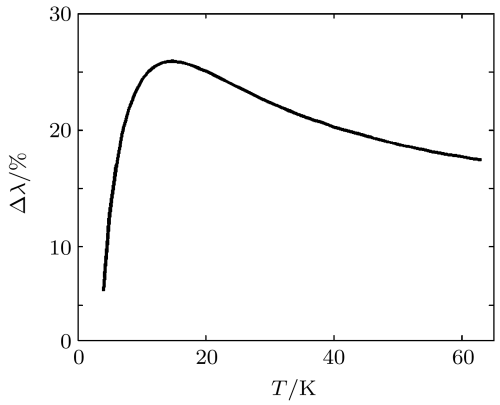


Fig. 7. The temperature-dependent relative difference of thermal conductivity $\Delta\lambda$ for isolated tube and bundles with the same chiral vector (5, 5).

5. Conclusions

In this paper, the phonon vibration modes are calculated by the force constant model and the results show that, due to the inter-tube van der Waals force, the number of low-energy phonon decreases in comparison with that of the corresponding isolated tube. Based on the obtained PDR and DOS, the thermal properties of bundles, including specific heat and thermal conductivity, have been studied. The influence of inter-tube interaction on the specific heat is mainly at extremely low temperatures and can be neglected in the high temperature range, where the specific heat of bundles is predominantly determined by the isolated tube itself. The inter-tube interaction leads to significant decrease of the low-temperature thermal conductivity of bundles and the maximum reduction can reach 26% around 17 K in comparison with that of isolated tube. Therefore, the effect of van der Waals interaction on the thermal conductivity at low temperature cannot be neglected.

References

[1] Iijima S 1991 *Nature* **354** 56
[2] Miao L, Liu H J, Hu Y, Zhou X, Hu C Z and Shi J 2010 *Chin. Phys.* B **19** 016301
[3] Kim P, Shi L, Majumdar A and McEuen L 2001 *Phys. Rev. Lett.* **87** 215502
[4] Fujii M, Zhang X, Xie H Q, Ago H, Takahashi K, Ikuta T, Abe H and Shimizu T 2005 *Phys. Rev. Lett.* **95** 065502
[5] Pop E, Mann D, Wang Q, Goodson K and Dai H J 2006 *Nano Lett.* **6** 96
[6] Berber S, Kwon Y K and Tomanek D 2000 *Phys. Rev. Lett.* **84** 4613
[7] Maruyama S, Kojima R, Miyauchi Y, Chiashi S and Kohno M 2002 *Chem. Phys. Lett.* **360** 229
[8] Mingo N and Broido D A 2005 *Phys. Rev. Lett.* **95** 096105
[9] Lindsay L, Broido D A and Mingo N 2009 *Phys. Rev.* B **80** 125407
[10] Choi S U S, Zhang Z G, Yu W, Lockwood F E and Grulke E A 2001 *Appl. Phys. Lett.* **79** 2252
[11] Fan S S, Chapline M G, Franklin N R, Tombler T W, Cassell A M and Dai H J 1999 *Science* **283** 512
[12] Andrews R, Jacques D, Rao A M, Derbyshire F, Qian D, Fan X, Dickey E C and Chen J 1999 *Chem. Phys. Lett.* **303** 467

[13] Pal S K, Son Y, Borca-Tasciuc T, Borca-Tasciuc D A, Kar S, Vajtai R and Ajayan P A 2008 *J. Mater. Res.* **23** 2099
[14] Gu H W and Swager T M 2008 *Adv. Mater.* **20** 4433
[15] Hone J, Batlogg B, Benes Z, Johnson A T and Fischer J E 2000 *Science* **289** 1730
[16] Xu J and Fisher T S 2006 *Int. J. Heat Mass Transfer* **49** 1658
[17] Kang J W, Song K O, Hwang H J and Jiang Q 2006 *Nanotechnology* **17** 2250
[18] Cox B J, Thamwattana N and Hill J M 2008 *Proc. R. Soc.* A **464** 691
[19] Thess A, Lee R, Nikolaev P, Dai H J, Petit P, Robert J, Xu C H, Lee Y H, Kim S G, Rinzler A G, Colbert D T, Scuseria G E, Tomanek D, Fischer J E and Smalley R E 1996 *Science* **273** 483
[20] Callaway J 1976 *Quantum Theory of the Solid State* (1st ed) (New York: Academic Press) pp. 1–52
[21] Satio R 1998 *Physical Properties of Carbon Nanotubes* (5th ed) (London: Imperial College Press) pp. 35–53
[22] Lu J P and Yang W T 1994 *Phys. Rev.* B **49** 11421
[23] Venkateswaran U D, Rao A M, Richter E, Menon M, Rinzler A, Smalley R E and Eklund P C 1999 *Phys. Rev.* B **59** 10928
[24] Kahn D and Lu J P 1999 *Phys. Rev.* B **60** 6535
[25] Popov V N, van Doren V E and Balkanski M 2000 *Phys. Rev.* B **61** 3078
[26] Tang J, Qin L C, Sasaki T, Yudasaka M, Matsushita A and Iijima S 2000 *Phys. Rev. Lett.* **85** 1887
[27] Hone J, Llaguno M C, Nemes N M, Johnson A T, Fischer J E, Walters D A, Casavant M J, Schmidt J and Smalley R E 2000 *Appl. Phys. Lett.* **77** 666
[28] Yamamoto T, Watanabe S and Watanabe K 2004 *Phys. Rev. Lett.* **92** 075502
[29] Xiao Y, Yan X H, Cao J X and Ding J W 2003 *J. Phys.*: *Condens. Matter* **15** L341
[30] Hone J ,Whitney M, Piskoti C and Zettl A 1999 *Phys. Rev.* B **59** R2514